New C_{84} Derivative and Its Application in a Bulk Heterojunction Solar Cell

Floris B. Kooistra,[†] Valentin D. Mihailetchi,[†] Lacramioara M. Popescu,[†] David Kronholm,[‡] Paul W. M. Blom,[†] and Jan C. Hummelen*[,†]

Molecular Electronics, Materials Science Centre Plus, University of Groningen, Nijenborgh 4, 9747 AG Groningen, The Netherlands, and Solenne B.V., Zernikepark 12, 9747 AN Groningen, The Netherlands

Received December 16, 2005. Revised Manuscript Received April 7, 2006

We report here the synthesis and characteristics of a new C_{84} adduct ([84]PCBM), realized via a diazoalkane addition reaction. [84]PCBM was obtained as a mixture containing three major isomers. [84]PCBM was tested in a fullerene/poly(2-methoxy-5-(3′,7′-dimethyloctyloxy)-*p*-phenylene vinylene) (MDMO-PPV) bulk heterojunction solar cell as the first C_{84} derivative to be applied in device fabrication. Spin coating the active layer blend from 1-chloronaphthalene (the very best fullerene solvent) instead of *ortho*-dichlorobenzene was necessary to obtain the more efficient photovoltaic device. The PV results indicate that the hole mobility of MDMO-PPV may *not* be increased upon blending with [84]PCBM. This explains the relatively low I_{SC} of the device as due to the buildup of space charge. The V_{OC} of the device is ∼500 mV lower than that of the one with [60]PCBM, while [84]PCBM has a 350 mV higher electron affinity than [60]PCBM. This loss surpasses the linear relation between the donor$_{HOMO}$−acceptor$_{LUMO}$ energy gap and the V_{OC} in this type of device. A maximum power conversion efficiency of 0.25% was reached for the MDMO-PPV:[84]PCBM cells.

Introduction

In 1991, soon after Krätschmer et al. first succeeded in isolating small quantities of C_{60}, the higher fullerene C_{84} was isolated as the third most abundant fullerene after C_{60} and C_{70}.[1,2] A total of 24 isomers of C_{84} obeying the isolated pentagon rule are predicted by calculations.[3] MNDO calculations furthermore predict that the two isoenergetic D_2 (22) and D_{2d} (23) isomers (numbers in accordance with the isomer numbering of Manolopoulos and Fowler)[3] are the most stable isomers by about 23 kJ mol^{-1} compared to the next stable ones.[4−7] Analysis of ^{13}C NMR spectra of C_{84}, obtained with the standard graphite arc process, is consistent with a 2:1 thermodynamic mixture of the isoenergetic D_2 and D_{2d} symmetry isomers.[8] This can also be interpreted as a 1:1:1 mixture becuase the D_2 isomer is chiral, and thus the two enantiomers are present in an equal amount. Interestingly these two isomers differ by only one Stone−Wales transformation.[9] By using metal-doped graphite rods in the carbon arc procedure, other isomers were obtained. Up until now 10 of the 24 isomers have been isolated.[10−13]

Since the isolation of C_{84} many efforts have been made to separate the isomeric mixture (D_2 and D_{2d}). Using an Ir(CO)Cl(PPh$_3$)$_2$ complex, Balch et al. succeeded in 1994 in separating the two major isomers and revealed the structure of the D_{2d} isomer by X-ray crystallography.[14] In the same year the kinetic resolution of the chiral D_2 isomer was published by Hawkins et al.[15] Later, separation by HPLC methods was successfully applied.[10] Another separation method using the Bingel-retro-Bingel strategy was applied by Crassous et al.[17]

As a result of the very limited availability of pure C_{84} only very few reactions have been carried out on this fullerene. So far most reactions on C_{84} were performed on a very small scale with the goal to separate the different isomers or to test the reactivity of C_{84}.[15−20] An important factor in reactions

* Corresponding author. E-mail: j c.hummelen@rug.nl. Fax: (+)31 503638751.
[†] University of Groningen.
[‡] Solenne B.V.

(1) Krätschmer, W.; Lamb, L. D.; Fostiropoulos, K.; Huffman, D. R. *Nature* **1990**, *347*, 354.
(2) Diederich, F.; Ettl, R.; Rubin, Y.; Whetten, R. L.; Beck, R.; Alvarez, M.; Anz, S.; Sensharma, D.; Wudl, F.; Khemani, K. C.; Koch, A. *Science* **1991**, *252*, 548.
(3) Manolopoulos, D. E.; Fowler, P. W. *J. Chem. Phys.* **1992**, *96*, 7603.
(4) Manolopoulos, D. E.; Fowler, P. W.; Taylor, R.; Kroto, H. W.; Walton, D. R. M. *J. Chem. Soc., Faraday Trans.* **1992**, *88*, 3117.
(5) Zhang, B. L.; Wang, C. Z.; Ho, K. M. *J. Chem. Phys.* **1992**, *96*, 7183.
(6) Bakowies, D.; Kolb, M.; Thiel, W.; Richard, S.; Ahlrichs, R.; Kappes, M. M. *Chem. Phys. Lett.* **1992**, *200*, 411.
(7) Raghavachari, K. *Chem. Phys. Lett.* **1992**, *190*, 397.
(8) Kikuchi, K.; Nakahara, N.; Wakabayashi, T.; Suzuki, S.; Shiromaru, H.; Miyake, Y.; Saito, K.; Ikemoto, I.; Kainosho, M.; Achiba, Y. *Nature* **1992**, *357*, 142.
(9) Stone, A. J.; Wales, D. J. *Chem. Phys. Lett.* **1986**, *128*, 501.
(10) Dennis, T. J. S.; Kai, T.; Tomiyama, T.; Shinohara, H. *Chem. Commun.* **1998**, 619.
(11) Dennis, T. J. S.; Kai, T.; Asato, K.; Tomiyama, T.; Shinohara, H.; Yoshida, T.; Kobayashi, Y.; Ishiwatari, H.; Miyake, Y.; Kikuchi, K.; Achiba, Y. *J. Phys. Chem. A* **1999**, *103*, 8747.
(12) Tagmatarchis, N.; Avent, A. G.; Prassides, K.; Dennis, T. J. S.; Shinohara, H. *Chem. Commun.* **1999**, 1023.
(13) Tagmatarchis, N.; Okada, K.; Yoshida, T.; Kobayashi, Y.; Shinohara, H. *Chem. Commun.* **2001**, 1366.
(14) Balch, A. L.; Ginwalla, A. S.; Lee, J. W.; Noll, B. C.; Olmstead, M. M. *J. Am. Chem. Soc.* **1994**, *116*, 2227.
(15) Hawkins, J. M.; Nambu, M.; Meyer, A. *J. Am. Chem. Soc.* **1994**, *116*, 7642.
(16) Wang, G. W.; Saunders: M.; Khong, A.; Cross, R. J. *J. Am. Chem. Soc.* **2000**, *122*, 3216.
(17) Crassous, J.; Rivera, J.; Fender, N. S.; Shu, L. H.; Echegoyen, L.; Thilgen, C.; Herrmann, A.; Diederich, F. *Angew. Chem., Int. Ed.* **1999**, *38*, 1613.

10.1021/cm052783z CCC: $33.50
Published on Web 06/02/2006

with C_{84} is the difference in reactivity of the various C═C double bonds. Whereas all double bonds are equivalent in C_{60}, this is not the case for higher fullerenes. In the case of C_{84} both isomers have 42 C═C double bonds, of which 6 are inter-pentagonal. Calculations by Taylor predict the highest π density for the D_2 isomer at the identical 9−10 and 17−18 inter-pentagonal double bonds and for the D_{2d} isomer at the identical 32−53 and 42−43 inter-pentagonal double bonds.[21] In case of the D_{2d} isomer this was experimentally shown by the selective formation of the $[(\eta^2-D_{2d}-C_{84})Ir(CO)Cl(PPh_3)_2]$ complex at the 32−53 bond.[14]

The intrinsic properties of C_{84} have been quite extensively investigated. Examples are the previously mentioned NMR spectroscopy, electrochemistry,[22] IR,[23−26] ionization energy,[27,28] and circular dichroism properties of the chiral isomers.[29,30] However, very little research has been done with respect to possible applications of C_{84}. A C_{84}-based field effect transistor was developed by Shibata et al.[31] Some pioneering work has been done in the field of nonlinear optics and superconductivity.[32−34]

Our recent successful application of the C_{70} derivative [70]PCBM as the alternative for [60]PCBM as the acceptor component in PCBM:MDMO-PPV (poly(2-methoxy-5-(3′,7′-dimethyloctyloxy)-*p*-phenylene vinylene)) bulk heterojunction solar cells, where we obtained 3.0% power conversion efficiency,[35] prompted us to prepare and evaluate an analogous C_{84} derivative. The improved performance of the [70]PCBM:MDMO-PPV solar cell, compared to the one based on the analogous [60]PCBM:MDMO-PPV active layer, is mainly due to its significantly broader and stronger absorption, which resulted in a higher current output. C_{84} has an even broader absorption than C_{70}, extending to the near infrared (NIR),[2,36] and, therefore, we expected a possible further improvement in the current output, especially when used in combination with a relatively wide band gap donor material like MDMO-PPV. An additional potential advantage of C_{84} as a component in molecular opto-electronic devices is its much larger photostability compared to C_{60} and C_{70}.[37] Triplet excited state formation upon photoexcitation is virtually absent in C_{84}, in sharp contrast to C_{60} and C_{70}. We consider this to be highly advantageous for the lifetime of the solar cell devices because we suspect one of the major degradation processes in organic solar cells to be singlet oxygen formation by quenching of the triplet exited state of the fullerene (i.e., the fullerene acting as a sensitizer in relatively large fullerene domains in which the initial singlet excited state is not effectively quenched by hole transfer to the donor but is allowed time for intersystem crossing to the triplet state).[37b]

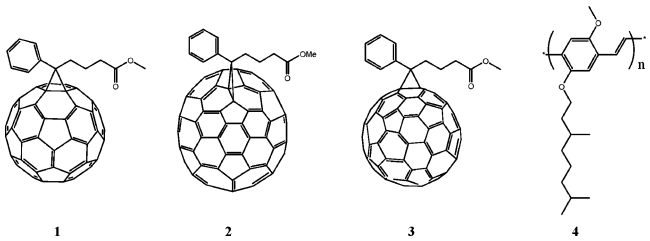

Figure 1. Structures of [60]PCBM **1**, [70]PCBM (major isomer) **2**, [84]PCBM (expected adduct to the D_{2d} isomer is shown) **3**, and MDMO-PPV **4**.

Here, we report on the preparation of the new C_{84} derivative [84]PCBM, on its application as an electron acceptor in a mixture with MDMO-PPV, and on a bulk heterojunction photovoltaic cell, made with such a mixture as the active layer. The structures of [60]PCBM, [70]PCBM, [84]PCBM, and MDMO-PPV are depicted in Figure 1. [84]PCBM was obtained as a mixture of three isomers, and it was used as such. The electron mobility in [84]PCBM appeared to be as high as that reported for the pristine fullerene.[31] Miscibility of the methanofullerenes with MDMO-PPV clearly diminishes with increasing size of the cage (i.e., [60]PCBM > [70]PCBM > [84]PCBM). Therefore, 1-chloronaphthalene was used as the spin-coat solvent for optimal functional morphology of the [84]PCBM:MDMO-PPV (4:1, w/w) blend. Despite the broader absorption spectrum of [84]PCBM, the maximum photovoltaic power conversion efficiency of the PV devices was a factor of 10−15 lower compared with similar [60]PCBM:MDMO-PPV and [70]PCBM:MDMO-PPV devices. The PV results indicate that the hole mobility of MDMO-PPV is *not* increased upon blending with [84]PCBM. As the main result hereof, the I_{SC} of the device is relatively low as a result of the build-up of space charge. The V_{OC} of the device is ∼500 mV lower than that of the one with [60]PCBM, while [84]PCBM has a 350 mV higher electron affinity than [60]PCBM. This

(18) Wakahara, T.; Han, A. H.; Niino, Y.; Maeda, Y.; Akasaka, T.; Suzuki, T.; Yamamoto, K.; Kako, M.; Nakadaira, Y.; Kobayashi, K.; Nagase, S. *J. Mater. Chem.* **2002**, *12*, 2061.
(19) Darwish, A. D.; Martsinovich, N.; Taylor, R. *Org. Biomol. Chem.* **2004**, *2*, 1364.
(20) Nuffer, R.; Bartl, A.; Dunsch, L.; Mathis, C. *Synth. Met.* **2001**, *121*, 1151.
(21) Taylor, R. *J. Chem. Soc., Perkin Trans. 2* **1993**, 813.
(22) Boulas, P. L.; Jones, M. T.; Ruoff, R. S.; Lorents, D. C.; Malhotra, R.; Tse, D. S.; Kadish, K. M. *J. Phys. Chem.* **1996**, *100*, 7573.
(23) Nishikawa, T.; Kinoshita, T.; Nanbu, S.; Aoyagi, M. *J. Mol. Struct.−THEOCHEM* **1999**, *462*, 453.
(24) von Helden, G.; Holleman, I.; Putter, M.; van Roij, A. J. A.; Meijer, G. *Chem. Phys. Lett.* **1999**, *299*, 171.
(25) Dennis, T. J. S.; Hulman, M.; Kuzmany, H.; Shinohara, H. *J. Phys. Chem. B* **2000**, *104*, 5411.
(26) Bettinger, H. F.; Scuseria, G. E. *Chem. Phys. Lett.* **2000**, *332*, 35.
(27) Steger, H.; Holzapfel, J.; Hielscher, A.; Kamke, W.; Hertel, I. V. *Chem. Phys. Lett.* **1995**, *234*, 455.
(28) Boltalina, O. V.; Ioffe, I. N.; Sidorov, L. N.; Seifert, G.; Vietze, K. *J. Am. Chem. Soc.* **2000**, *122*, 9745.
(29) Fanti, M.; Orlandi, G.; Poggi, G.; Zerbetto, F. *Chem. Phys.* **1997**, *223*, 159.
(30) Furche, F.; Ahlrichs, R. *J. Am. Chem. Soc.* **2002**, *124*, 3804.
(31) Shibata, K.; Kubozono, Y.; Kanbara, T.; Hosokawa, T.; Fujiwara, A.; Ito, Y.; Shinohara, H. *Appl. Phys. Lett.* **2004**, *84*, 2572.
(32) Harigaya, K. *J. Lumin.* **1998**, *76−77*, 652.
(33) Denning, M. S.; Dennis, T. J. S.; Rosseinsky, M. J.; Shinohara, H. *Chem. Mater.* **2001**, *13*, 4753.
(34) Koudoumas, E.; Konstantaki, M.; Mavromanolakis, A.; Michaut, X.; Couris, S.; Leach, S. *J. Phys. B: At. Mol. Opt. Phys.* **2001**, *34*, 4983.
(35) Wienk, M. M.; Kroon, J. M.; Verhees, W. J. H.; Knol, J.; Hummelen, J. C.; van Hal, P. A.; Janssen, R. A. J. *Angew. Chem., Int. Ed.* **2003**, *42*, 3371.
(36) Ajie, H.; Alvarez, M. M.; Anz, S. J.; Beck, R. D.; Diederich, F.; Fostiropoulos, K.; Huffman, D. R.; Krätschmer, W.; Rubin, Y.; Schriver, K. E.; Sensharma, D.; Whetten, R. L. *J. Phys. Chem.* **1990**, *94*, 8630.
(37) (a) Juha, L.; Ehrenberg, B.; Couris, S.; Koudoumas, E.; Leach, S.; Hamplova, V.; Pokorna, Z.; Mullerova, A.; Kubat, P. *Chem. Phys. Lett.* **2001**, *335*, 539. (b) Hummelen, J. C.; Knol, J.; Sánchez, L. *Proc. SPIE-Int. Soc. Opt. Eng.* **2001**, *4108*, 76.

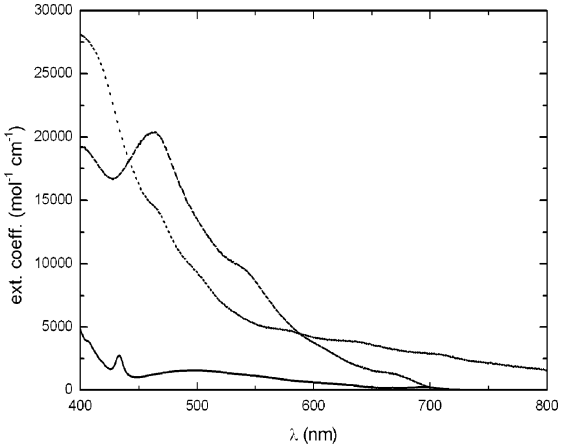

Figure 2. UV/vis spectra of [84]PCBM (dotted line), [70]PCBM (dashed line), and [60]PCBM (straight line), all in toluene.

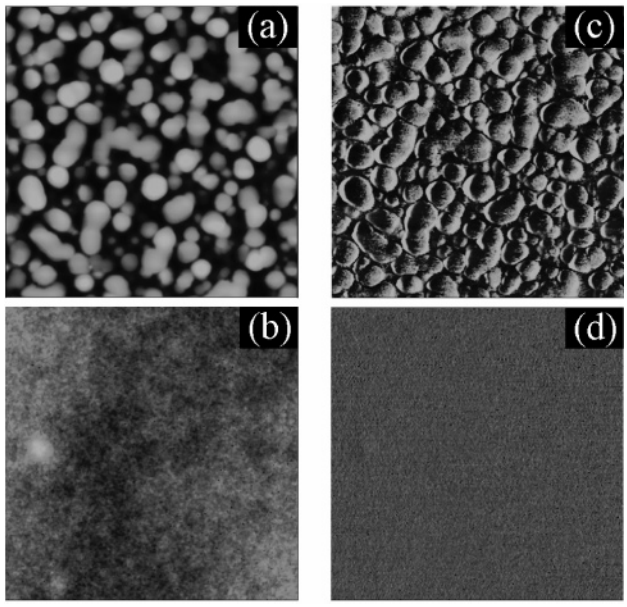

Figure 3. AFM tapping-mode height (a, b) and simultaneously taken phase (c, d) images of [84]PCBM:MDMO-PPV (4:1, w/w) blends, with a size of 5.0 μm × 5.0 μm. The films are spin-coated from ODCB (a, c; z range = 180 nm, RMS roughness = 12.16 nm) and 1-chloronaphthalene (b, d; z range = 10 nm, RMS roughness = 0.88 nm).

loss surpasses the linear relation between the donor$_{HOMO}$−acceptor$_{LUMO}$ energy gap and the V_{OC} in this type of device.

Experimental Section

Device Preparation. The solar cell devices were prepared using indium tin oxide (ITO) coated glass substrates. To supplement this bottom electrode, a hole transport layer of poly(3,4-ethylenedioxythiophene)−poly(styrene sulfonic acid) (PEDOT−PSS; Bayer AG) was spun from an aqueous dispersion solution, under ambient conditions, before drying the substrates at 140 °C for 10 min. Next, the photoactive layer consisting of [84]PCBM:MDMO-PPV (4:1, w/w) was spin-coated from either *ortho*-dichlorobenzene (ODCB) or 1-chloronaphthalene solution on top of the PEDOT:PSS layer in the N_2 atmosphere. To complete the solar cell devices, 1 nm of lithium fluoride (LiF), topped with aluminum (Al, 100 nm) electrodes, was deposited by thermal evaporation under vacuum ($<10^{-7}$ mbar). The active layer thickness in the various devices is given in Figure 4.

Device Measurements. The current density versus voltage curves were measured in a N_2 atmosphere (<1 ppm O_2 and <1 ppm H_2O) at room temperature with a computer-controlled Keithley 2400 Source Meter. To measure the photocurrent (J_L), the devices were illuminated at the transparent ITO electrode by a white light tungsten−halogen lamp, with a spectral range of 400−800 nm, calibrated against a calibrated Si diode to an intensity of 82 mW/cm^2 (0.82 Sun illumination). Atomic force microscope (AFM) images were recorded on an ITO/PEDOT:PSS covered-glass substrate, with a DI NanoScope IV AFM operating under ambient conditions in tapping mode.

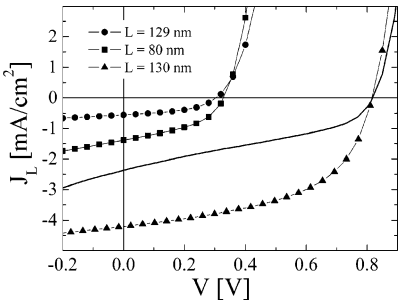

Figure 4. Current density−voltage characteristics under illumination (J_L) of [84]PCBM:MDMO-PPV (4:1, w/w) devices, spin-coated from ODCB (●) and 1-chloronaphthalene (■), together with a [60]PCBM:MDMO-PPV (4:1, w/w) device spin-coated from CB (▲), used here as a reference. The devices thicknesses (L) are provided in the figure. The solid line represents the experimental data of the [84]PCBM:MDMO-PPV device in 1-chloronaphthalene (■), scaled for the same V_{OC} as the reference device. All devices were illuminated using a tungsten/halogen lamp with a spectral range of 400−800 nm, calibrated to an intensity of 82 mW/cm^2.

Materials. All reagents and solvents were used as received or purified using standard procedures. Combustion produced [84]fullerene (98%) was supplied by Nano-C, Inc. (33 Southwest Park, Westwood, MA 02090, U.S.A.) and used without further purification. Flash chromatography was performed using silica gel (Kieselgel Merck Type 9385 (230−400 mesh)). ^{1}H NMR and ^{13}C NMR were performed on a Varian Unity Plus (400 MHz), at 298 K. IR measurements were performed on a Nicolet Nexus FT-IR instrument. UV/vis was performed on a Perkin-Elmer Instruments Lambda 900 spectrometer. HPLC analyses were performed on a Hewlett-Packard HPLC−Chemstation 3D (HP 1100 Series) using an analytical Cosmosil Buckyprep column (4.6 × 250 mm). As a solvent cyclohexane/toluene (1:1) was used with a flow rate of 1 mL/s. Cyclic voltammetry (CV) and differential pulse voltammetry (DPV) were performed using an Autolab PGStat 100.

Synthesis and Characterization of [84]PCBM. A flame dried 100 mL three-necked flask, equipped with a stirring egg, thermometer, N_2 inlet, and condenser, was charged with 4-benzoylmethylbutyrate *p*-tosylhydrazone (55.2 mg, 0.147 mmol, 1.07 equiv), NaOMe (8.2 mg, 0.152 mmol, 1.1 equiv), and dry pyridine (2 mL). The resulting mixture was stirred for 1.5 h. To the mixture was added a solution of C_{84} (139 mg, 0.138 mmol) in ODCB (25 mL). The resulting mixture was heated to 80 °C, and irradiation was started with a 150 W Na lamp. The irradiation was stopped after ~4 h. All pyridine was evaporated in vacuo, and the remaining mixture was purified by column chromatography. Elution with CS_2 yielded unreacted C_{84}. Subsequent elution with cyclohexane/toluene (1:1) yielded the monoadduct fraction. Both fractions were evaporated to dryness, and the residues were dissolved in a minimal amount of ODCB and precipitated with MeOH. The resulting suspensions were centrifuged, and the MeOH was decanted. The resulting brown pellets were washed twice with MeOH, centrifuged, and decanted. The obtained brown pellets were dried at 50 °C in vacuo for 2 days. Isolated yields: recovered C_{84}, 48.6 mg (4.8 × 10^{-2} mmol, 35%). Monoadduct (isomeric mixture): 37.5 mg (3.12 × 10^{-2} mmol, 23%). Isomer assignment is based on observed intensity variation among signals in different batches. The presented

spectroscopic data is that of combined [84]PCBM batches. IR (KBr) ν (cm^{-1}): 2942 (m), 1737 (s), 1628 (m), 1600 (w), 1517 (w), 1493 (w), 1455 (s), 1434 (s), 1384 (m), 1330 (m), 1261 (m), 1155 (m), 1056 (w), 1034 (s), 795 (s), 749 (s), 727 (w), 702 (s), 643 (s), 576 (m), 527 (w), 515 (w), 499 (m), 455 (w), 432 (w), 426 (w), 415 (w), 405 (w). ^{1}H NMR (CS_2/D_2O, 400 MHz) δ: 8.0 (d, $J = 7.0$ Hz), 7.89 (d, $J = 6.6$ Hz), 7.58−7.41 (m), 7.26−7.23 (m), 3.65 (s) (isomer A and C), 3.63 (s) (isomer B), 3.47 (m) (isomer A), 3.27 (m) (isomer C), 3.09 (t, $J = 8.1$ Hz) (isomer C), 2.54 (t, $J = 7.3$ Hz) (isomer A), 2.49 (t, $J = 7.3$ Hz) (isomer B), 2.28−2.22 (m). ^{13}C NMR (CS_2, 100 MHz) δ (ppm): 170.86, 170.80, 153.74, 151.57, 151.47, 151.29, 150.72, 149.95, 149.83, 143.57, 143.51, 143.09, 142.86, 142.56, 142.50, 142.16, 141.65, 141.45, 140.97, 140.90, 140.62, 140.57, 140.33, 140.31, 138.82, 138.78, 137.97, 137.93, 137.89, 137.47, 137.46, 137.33, 137.28, 137.23, 137.15, 137.01, 136.37, 135.77, 134.56, 134.50, 133.34, 133.07, 132.05, 131.94, 131.62, 130.02, 128.13, 128.08, 127.97, 127.84, 127.04, 64.75, 61.98, 61.74, 54.12, 50.83, 50.65, 50.62, 50.53, 37.23, 35.58, 35.05, 34.91, 34.78, 34.46, 33.88, 33.30, 33.26, 33.08, 33.03, 32.89, 29.75, 28.65, 26.37, 22.93, 22.84, 22.56, 21.86, 21.69, 21.37, 20.95, 20.69, 20.15. HPLC retention times (min): 8.77, 9.15, 10.16.

Results and Discussion

The synthetic procedure for [84]PCBM, as described in the experimental part of this paper, yielded a mixture of isomeric monoadduct methanofullerenes. The formation of a *minimum* of two [84]PCBM isomers was to be expected because the C_{84} itself consists of two isomers.[38] Three major isomers were clearly distinguished in the ^{1}H NMR spectrum of the product. At 3.46 ppm a triplet with a small secondary coupling was seen, next to an identical pattern of smaller intensity at 3.27 ppm, and a third such triplet is partly hidden underneath the methoxy signals at ~3.65 ppm. Such a pattern is typical for the protons on the methylene group next to the cyclopropane moiety in PCBX type methanofullerenes. Two signals were observed at 3.65, and 3.63 ppm, respectively, of which one was of high intensity and one was of low intensity for the OCH_3 group. Three $-CH_2COOR$ triplets can be seen at 3.09 (minor), 2.54 (major), and 2.49 (minor) ppm. In the ^{13}C spectrum only two carbonyl resonances were observed separately, namely, at 170.86 and 170.80 ppm. Furthermore, three bridgehead carbon signals were observed at 64.75, 61.98, and 61.74 ppm, again indicating the presence of three isomers. Considering both proton and carbon NMR data, we conclude that the product consists of three [84]PCBM isomers. This conclusion was further supported by an HPLC trace, in which three peaks were observed.

To test the electron accepting properties of [84]PCBM, CV and DPV experiments were performed. A comparison was made with [60]PCBM and [70]PCBM.

From both experiments it can be concluded that [84]PCBM is a much better electron acceptor than [60]PCBM and [70]PCBM by about 350 mV. This immediately implies that the maximum open circuit voltage that can be obtained with solar cell devices constructed with [84]PCBM as the acceptor and MDMO-PPV as the donor will be dramatically lower compared to the ones based on [60]PCBM and [70]PCBM, because the maximum open circuit voltage that can be obtained is directly correlated to the energy difference between the HOMO of the donor and the LUMO of the acceptor.[39,40] Despite the expectation of a reduced V_{OC}, we were interested in the photocurrent increase due to the enhanced absorption of [84]PCBM. The UV−vis absorption spectrum of the isomeric [84]PCBM mixture is shown in Figure 2. It appears that the absorption of [70]PCBM and [84]PCBM is much stronger than that of [60]PCBM. Furthermore, in the area of 630−800 nm, where [60]PCBM and [70]PCBM are very close to transparent, [84]PCBM still shows a significant absorption. Hence, a better match with the AM 1.5 solar spectrum is observed for [84]PCBM, but the molar absorption in the 400−500 range is somewhat weaker than that of [70]PCBM.

It must be kept in mind, however, that the photovoltaic performance of a bulk heterojunction type solar cell is also strongly dependent on the morphology of the composite active layer.[41] Efficient charge generation and transport strongly relate to even dispersion of PCBM and PPV in the mixture. Because larger fullerenes tend to be less soluble, processing of higher fullerenes becomes increasingly more difficult. The fact that for optimal processing conditions [60]PCBM:MDMO-PPV solar cells are spun from chlorobenzene (CB) and [70]PCBM:MDMO-PPV solar cells are spun from ODCB is illustrative.[35,41] Therefore, the choice of solvent is a critical parameter in obtaining the best photovoltaic performance. Tapping-mode atomic force microscopy was employed to investigate the structure of the different [84]PCBM:MDMO-PPV (4:1, w/w) mixtures. The "standard" weight ratio of 4:1 was used, because (a) this results in a comparable volume ratio of donor and acceptor components in the three blends; (b) the same ratio was used in the optimized cells with [60]PCBM and [70]PCBM. It is expected that there is no significant difference between bulk and surface morphologies as confirmed by investigating the morphology at different depths in the case of [60]PCBM:MDMO-PPV blends.[42] Figure 3 shows the height and corresponding phase images obtained by AFM for composite films of [84]PCBM:MDMO-PPV, fabricated from two different solvents: ODCB and the best fullerene solvent, that is, 1-chloronaphthalene. To match the conditions used for the device preparation, the films studied here were spin-coated on ITO substrates covered with an additional layer of PEDOT−PSS which forms the bottom hole injection electrode of the photovoltaic device. The height images of the films fabricated from ODCB reveal an extremely uneven surface with a reproducible phase contrast, which clearly indicates that the "peaks" are of a different chemical nature than the surrounding "valleys". Separate domains of one phase in a matrix of another phase can be easily recognized,

(38) According to HPLC analysis, the combustion produced C_{84} we used consisted of approximately 80% D_{2d} isomer and 20% D_2 isomer.

(39) Brabec, C. J.; Cravino, A.; Meissner, D.; Sariciftci, N. S.; Fromherz, T.; Rispens, M. T.; Sanchez, L.; Hummelen, J. C. *Adv. Funct. Mater.* **2001**, *11*, 374.
(40) Brabec, C. J.; Cravino, A.; Meissner, D.; Sariciftci, N. S.; Rispens, M. T.; Sanchez, L.; Hummelen, J. C.; Fromherz, T. *Thin Solid Films* **2002**, *403*, 368.
(41) Shaheen, S. E.; Brabec, C. J.; Sariciftci, N. S.; Padinger, F.; Fromherz, T.; Hummelen, J. C. *Appl. Phys. Lett.* **2001**, *78*, 841.
(42) van Duren, J. K. J.; Yang, X.; Loos, J.; Bulle-Lieuwma, C. W. T.; Sieval, A. B.; Hummelen, J. C.; Janssen, R. A. J. *Adv. Funct. Mater.* **2004**, *14*, 425.

with feature sizes of approximately 200−400 nm and a root-mean-square (RMS) roughness of 12.16 nm for 5.0 μm × 5.0 μm sampling areas. Conversely, the samples fabricated from 1-chloronaphthalene show extremely smooth surfaces with a RMS roughness of 0.88 nm and domain sizes ranging from 20 to 50 nm for the same size of sampling area. Because the exciton diffusion length in organic materials is typically small (∼10 nm), such small size features favor exciton separation and subsequently yield a higher photocurrent. Thus, from the standpoint of morphology, the [84]PCBM:MDMO-PPV devices when prepared with 1-chloronaphthalene reveal the same features as their predecessors [70]PCBM and [60]PCBM fabricated from ODCB and CB, respectively.[35,41]

The large differences in the film morphology of [84]PCBM:MDMO-PPV are also reflected in the photovoltaic behavior of the cells. The solar cells were made by sandwiching the [84]PCBM:MDMO-PPV mixture between two electrodes with a different work function to generate an electric field over the active layer, necessary to separate and transport the photogenerated charge carriers. A transparent ITO/PEDOT:PSS high-work function bottom electrode was employed to collect holes, and LiF/Al as a low-work function electrode was used for electron collection. Moreover, it is demonstrated that the PEDOT:PSS favor an ohmic contact for holes to MDMO-PPV and LiF/Al forms an Ohmic contact for electrons to PCBM.[43] Under these circumstances, the V_{OC} of these devices is maximized and limited by the difference between the LUMO of the PCBM acceptor and the HOMO of the PPV donor.[39,40,43] The solar cell devices were illuminated with a tungsten/halogen lamp, with a spectral range of 400−800 nm, calibrated to an intensity approximately equivalent to 0.82 suns (82 mW/cm^2). To compare the impact of [84]PCBM on the photovoltaic device performance, reference devices of [60]PCBM:MDMO-PPV (4:1, w/w) were fabricated and characterized in an identical manner except for the choice of solvent (CB) used for spin-coating the active layer.[41] Figure 4 shows the current density−voltage characteristics under illumination (J_L) of the [84]PCBM:MDMO-PPV (4:1, w/w) devices, fabricated from ODCB and 1-chloronaphthalene. After averaging a number of devices, the V_{OC} values of the cells are 317 ± 7.6 mV in the case of ODCB and 335 ± 5.4 mV for 1-chloronaphthalene based devices. Although slightly higher in 1-chloronaphthalene, the V_{OC} of [84]PCBM based solar cells is a factor of 2.5 lower than that obtained in the similar [60]PCBM devices (819 ± 8.2 mV), as inferred from Figure 4. The dramatically lower V_{OC} of the [84]PCBM cells relative to [60]PCBM originates from the difference in their LUMO levels, although not fully accounted for by the CV and DPV measurements shown in Table 1.

On the other hand, the short-circuit current density (J_{SC}) of [84]PCBM:PPV devices strongly depends on the spin-coat solvent, and it exhibits more than a 2-fold increase when the blend is spun from 1-chloronaphthalene (1.38 ± 0.004 mA/cm^2) compared with ODCB (0.59±0.036 mA/cm^2). This is a result of an enhanced generation rate of charge carriers due to an increased donor/acceptor interface area, which facilitates exciton dissociation. Furthermore, the J_{SC} of the best [84]PCBM:MDMO-PPV device is more than a factor of 3 lower than that of the reference [60]PCBM-based device, despite an increased optical density of the blend when using [84]PCBM. Moreover, the fill factors (FF)[44] of the devices made with [84]PCBM are smaller compared with those of the reference [60]PCBM containing device (44.6 ± 2.1% vs 56.4 ± 2.8%). Consequently, the overall power conversion efficiency (η)[45] of [84]PCBM:MDMO-PPV is only 0.25%, being approximately 10-fold lower than the η measured in the [60]PCBM:MDMO-PPV devices, under the same experimental conditions.

Table 1. CV/DPV Data

	CV		DPV	
compound[a]	$E^{1/2}$ 1, red (V)	$E^{1/2}$ 2, red (V)	$E^{1/2}$ 1, red (V)	$E^{1/2}$ 2, red (V)
[60]PCBM	−1.078	−1.475	−1.084	−1.480
[70]PCBM[b]	−1.089	−1.479	−1.096	−1.479
[84]PCBM[b]	−0.730	−1.054	−0.736	−1.067

[a] Experimental conditions: V vs Fc/Fc^+, Bu_4NPF_6 (0.1 M) as the supporting electrolyte, ODCB/CH_3CN (4:1) as the solvent; scan rate, 10 mV/s. [b] Isomeric mixture.

The most important parameter that limits the η of [84]PCBM:MDMO-PPV devices is V_{OC}. Recently, we have addressed the relationship between V_{OC} and the remaining solar cell parameters (as J_{SC}, η, and FF) in [60]PCBM:MDMO-PPV devices.[46] We have demonstrated that when the photocurrent is scaled for the effective applied voltage on the device, given by $V_{OC}-V$, it shows a universal behavior, allowing from this the prediction of the other solar cell parameters. In other words, a decrease in the V_{OC} of the cell triggers a drop in both J_{SC} and FF, which subsequently strongly reduces the η.[45] Therefore, a correct comparison can be done only when both the [84]PCBM and the reference [60]PCBM devices are scaled for the same effective applied voltage ($V_{OC}-V$). The solid line in Figure 4 represents the experimental data of the [84]PCBM:MDMO-PPV device from 1-chloronaphthalene (■), scaled for the same V_{OC} as the reference [60]PCBM device. It can be seen that the J_{SC} value of the [84]PCBM is not entirely explained by the lower V_{OC}. Although the [84]PCBM shows a significantly higher absorption coefficient in the visible region compared with [60]PCBM, as indicated in Figure 2, the J_{SC} is still a factor of 1.7 lower after rescaling.

An important question remains on why such a low photocurrent is generated in the [84]PCBM-MDMO-PPV devices. Obviously, applying a lower band gap acceptor, like [84]PCBM, is only of use if the excitation of [84]PCBM also contributes efficiently to the photocurrent generation in the solar cells. Therefore, we compared the action spectrum of a MDMO-PPV:[60]PCBM cell with that of a MDMO-PPV:[84]PCBM cell, the latter with the active layer spun

(43) Mihailetchi, V. D.; Blom, P. W. M.; Hummelen, J. C.; Rispens, M. T. *J. Appl. Phys.* **2003**, *94*, 6849.

(44) The FF is defined as FF[%] = ($J_M \times V_M \times 100$)/($J_{SC} \times V_{OC}$), where J_M and V_M are current density and voltage at the maximum power point, respectively.

(45) The power conversion efficiency is defined as η[%] = ($J_{SC} \times V_{OC} \times$ FF)/P_{in}, where P_{in} represents the incident light power.

(46) Mihailetchi, V. D.; Koster, L. J. A.; Blom, P. W. M. *Appl. Phys. Lett.* **2004**, *85*, 970.

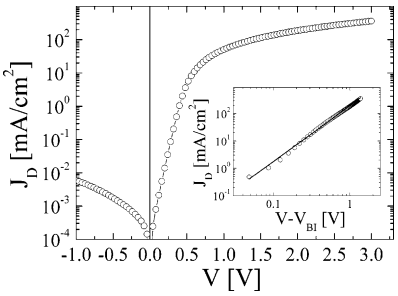

Figure 5. Dark current density−voltage characteristics (J_D) of an ITO/PEDOT:PSS/[84]PCBM:MDMO-PPV(4:1, w/w)/LiF/Al diode with the thickness of 129 nm at a temperature $T = 295$ K. The inset shows the $\log(J_D)-\log(V)$ characteristic corrected for the built-in voltage ($V_{BI} = 0.31$ V), together with the calculated SCLC (solid line).

from ODCB. Although the morphology of the latter cell appeared far from optimal later on during this study, comparing the action spectra of both cells in a normalized way clearly indicated that the [84]PCBM cell shows a significant portion of the action up to beyond a 900 nm wavelength, parallel to the absorption spectrum of [84]PCBM. Another important parameter that could limit the device performance is the charge carrier mobility. We have recently demonstrated that the most important factor in obtaining 2.5% efficiencies in [60]PCBM:MDMO-PPV is the enhancement, by more than 2 orders of magnitude, of the hole mobility of MDMO-PPV inside that blend.[47] Additionally, despite such a strong enhancement of the hole transport in the blend, the dark current density (J_D) of the solar cell devices is still dominated by the electron transport through the [60]PCBM phase,[48] being at least 1 order of magnitude higher. Accordingly, we estimate the electron mobility in the fullerene phase of the [84]PCBM-MDMO-PPV blend in the following manner. Figure 5 shows the experimental J_D-V characteristics of an ITO/PEDOT:PSS/[84]PCBM:MDMO-PPV (4:1, w/w)/LiF/Al diode with thickness of 129 nm, at room temperature. The slope of the $\log(J_D)-\log(V - V_{BI})$ plot, shown in the inset of Figure 5, indicates that J_D depends quadratically on the voltage, which is characteristic for the space-charge limited current (SCLC).[48,49]

From the fit of the SCLC to the experimental data (solid line) we have been able to extract an electron mobility, in the [84]PCBM phase, on the order of 1.0×10^{-3} cm^2/(V s), being consistent with the mobility found in commercially available C_{84}.[31,50] The high electron mobility in [84]PCBM, which is comparable with that of [60]PCBM,[49] clearly indicates that the electron transport in the [84]PCBM phase does not limit the performance of these [84]PCBM:MDMO-PPV devices. Another reason for the poor performance might be the presence of a large mobility difference between the electron and the holes in a [84]PCBM:MDMO-PPV blend. We recently have demonstrated that the photocurrent in PPV:PCBM devices can be limited by the space charge when the difference between the electron and the hole mobility exceeds 2 orders of magnitude.[51] A photocurrent of a device limited by the space charge is the maximum electrostatically allowed current that can be generated into the external circuit, and it has a strong impact on FF and J_{SC} of the respective solar cell. The typical FF of space-charge limited solar cells is close to 42%.[51] The FF of 44% in the [84]PCBM:MDMO-PPV cells is very close to this space-charge limited value, indicating that these cells are indeed limited by the buildup of space charge. A possible reason would be that, in contrast to [60]PCBM:MDMO-PPV blends, the hole mobility of the MDMO-PPV is not as strongly enhanced when blended with [84]PCBM. This will be a subject of further investigations.

Conclusions

We successfully performed a 1,3 dipolar addition reaction on C_{84} (as a 4:1 mixture of the D_2 and a D_{2d} isomers), obtaining a mixture of three [84]PCBM isomers, as most clearly indicated by NMR and HPLC data. [84]PCBM is a better electron acceptor then [60]PCBM and [70]PCBM by ~350 mV, as determined electrochemically. This, in combination with the known photostability of [84]fullerene, makes [84]PCBM an interesting new material for various molecular electronics applications. Here, we applied this new methanofullerene as an electron acceptor in a bulk heterojunction organic solar cell device with MDMO-PPV as the electron donor component. The diminished solubility of [84]-PCBM resulted in undesirable morphologies of the active layer when the 4:1 mixture was spun from ODCB. However, spin coating the mixture from the best fullerene solvent 1-chloronaphthalene gave smooth films and a concomitant 2-fold increase of the current output. In accord with the NIR absorption of [84]PCBM, the action spectrum of the PV devices was extended up to beyond 900 nm. However, as a result of the low V_{OC} of the devices, in combination with a low I_{SC}, the overall efficiency was limited to 0.25%. The combination of the electron mobility in the [84]PCBM phase being only slightly lower than that of [60]PCBM in blends with MDMO-PPV and the FF of 0.44 and relatively very low I_{SC} of the [84]PCBM:MDMO-PPV cells point to the explanation that the hole mobility in the MDMO-PPV phase of the [84]PCBM:MDMO-PPV blend may *not* be enhanced by this methanofullerene. Nevertheless, [84]PCBM remains a potentially very useful acceptor material for bulk heterojunction application, namely, when applied in combination with a more miscible and weaker donor than MDMO-PPV.

CM052783Z

(47) Melzer, C.; Koop, E. J.; Mihailetchi, V. D.; Blom, P. W. M. *Adv. Funct. Mater.* **2004**, *14*, 865.
(48) van Duren, J. K. J.; Mihailetchi, V. D.; Blom, P. W. M.; van Woudenbergh, T.; Hummelen, J. C.; Rispens, M. T.; Janssen, R. A. J.; Wienk, M. M. *J. Appl. Phys.* **2003**, *94*, 4477.
(49) Mihailetchi, V. D.; van Duren, J. K. J.; Blom, P. W. M.; Hummelen, J. C.; Janssen, R. A. J.; Kroon, J. M.; Rispens, M. T.; Verhees, W. J. H.; Wienk, M. M. *Adv. Funct. Mater.* **2003**, *13*, 43.
(50) The source and composition of the C_{84} used by the authors in ref 31 is not disclosed.
(51) Mihailetchi, V. D.; Wildeman, J.; Blom, P. W. M. *Phys. Rev. Lett.* **2005**, *94*, 126602.